Stability Analysis of Mechanical Seals With Two Flexibly Mounted Rotors

J. Wileman

Laboratoire de Mécanique des Solides,
URA CNRS Université de Poitiers,
Poitiers, France

I. Green

The George W. Woodruff School of
Mechanical Engineering,
Georgia Institute of Technology,
Atlanta, GA 30332

Dynamic stability is investigated for a mechanical seal configuration in which both seal elements are flexibly mounted to independently rotating shafts. The analysis is applicable to systems with both counterrotating and corotating shafts. The fluid film effects are modeled using rotor dynamic coefficients, and the equations of motion are presented including the dynamic properties of the flexible support. A closed-form solution for the stability criteria is presented for the simplified case in which the support damping is neglected. A method is presented for obtaining the stability threshold of the general case, including support damping. This method allows instant determination of the stability threshold for a fully-defined seal design. A parametric study of an example seal is presented to illustrate the method and to examine the effects of various parameters in the seal design upon the stability threshold. The fluid film properties in the example seal are shown to affect stability much more than the support properties. Rotors having the form of short disks are shown to benefit from gyroscopic effects which give them a larger range of stable operating speeds than long rotors. For seals with one long rotor, counterrotating operation is shown to be superior because the increased fluid stiffness transfers restoring moments from the short rotor to the long.

Introduction

In most face seal applications, a single rotating element (the rotor) is separated by a thin film of the sealed fluid from a nonrotating element (the stator). These seals usually have either of two basic configurations. In the flexibly mounted stator (FMS) configuration the stator is attached to the seal housing by means of a flexible support and anti-rotation locks, and the rotor is rigidly mounted to its shaft (Green and Etsion, 1985). Conversely, in the flexibly mounted rotor (FMR) configuration the stator is rigidly mounted to the seal housing while the rotor is attached to the shaft by means of a flexible support and positive drive devices (Metcalfe, 1981 and Green, 1989 and 1990). In either case, the rigid element will have misalignments which result from manufacturing imperfections, and the purpose of the flexible support is to allow the flexibly mounted element to track the misalignments in the rigidly mounted element. This decreases the relative misalignment, which in turn reduces the leakage and decreases the probability of face contact. Dynamic investigations of seals having either the FMS or FMR configuration date back almost three decades. Extensive literature reviews have been provided by Allaire (1984), Tournerie and Frêne (1985), and Etsion (1982, 1985, and 1991).

Wileman and Green (1991, 1996, 1997) have described a configuration in which both elements are flexibly mounted to rotating shafts, denoting it FMRR (Fig. 1). Such seals could be used for sealing between two rotating shafts for applications such as interstage seals in gas turbine engines (Miner, 1992) where counterrotating rotors are used to increase the power-to-weight ratio.

The fluid film between the faces of a noncontacting seal transmits forces and moments between the elements and couples their dynamic responses. These forces and moments result from the fluid pressure in the film, which is governed by the Reynolds equation. In order to determine the dynamic response of such a fluid-coupled system, it is normally necessary to solve the equations of motion simultaneously with the equations which govern the fluid behavior. The problem requires an iterative, numerical solution such as that provided by Green and Etsion (1986) for the FMS configuration.

Green and Etsion (1983) have introduced an alternate method of modeling the dynamic properties of the fluid film using linearized rotor dynamic coefficients. Expressions for the forces and moments applied by the fluid film are obtained by solving the Reynolds equation for an FMS seal. Derivatives of these forces and moments are then computed assuming small motions about an equilibrium position. The technique assumes an incompressible and isoviscous sealed fluid and uses small angle approximations. These equivalent stiffness and damping coefficients allow the fluid behavior to be introduced directly into the equations of motion. Using this technique, Green and Etsion (1985) determined the stability criteria and steady-state response for the FMS configuration, and Green (1987, 1989, and 1990) extended the results to the FMR configuration. Wileman and Green (1991, 1997) obtained the rotor dynamic coefficients for the FMRR configuration, then derived the equations of motion and developed a method to determine the steady-state response of the system.

This work analyzes the equations of motion derived by Wileman and Green (1997) to provide a solution for the stability limits of the FMRR configuration. The resulting stability criteria predict whether a seal will fail because of face contact or excessive leakage resulting from dynamic instability. Although this work is concerned exclusively with smooth-face seals, the analysis presented here can be extended to more complex seal face geometries, such as wavy or grooved faces, but for seals which do not have smooth faces the rotor dynamic coefficients may have to be computed numerically (e.g., Person et al., 1997).

Kinematic Description and Equations of Motion

Green (1990) showed that the axial vibrations in an FMR seal are decoupled from the angular modes, so that the solutions for the axial modes can be obtained independently. Wileman and Green (1991) showed that this decoupling extends to the
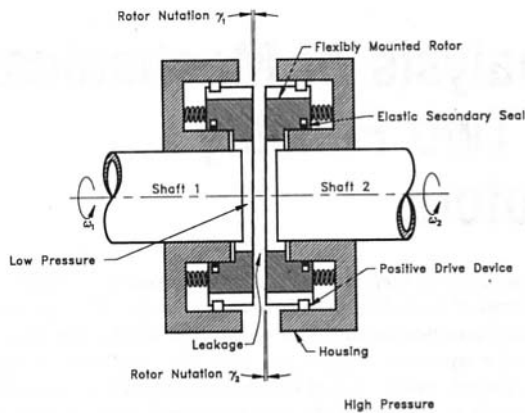
Fig. 1 Schematic of an FMRR mechanical seal

FMRR configuration, so that axial stability is assured so long as the axial fluid film stiffness is positive. Therefore, this work will focus exclusively on the stability in the angular modes.

The equations of motion for the seal elements are a moment balance between the dynamic moments and the moments applied by both the flexible support and the fluid film. The kinematic model necessary to obtain these equations of motion has been described in detail by Wileman and Green (1991), and is illustrated in Figs. 2 and 3. For clarity in the description, the two flexibly mounted rotors in the seal are denoted elements 1 and 2, but either element may be initially assigned either number so long as the assignment is used consistently throughout the analysis. Figure 2 shows the inertial reference frame, $\xi\eta\zeta$, and the principal systems for both elements, denoted $x_n y_n z_n$ where the subscript n indicates either rotor 1 or 2. Figure 3 is a vector diagram showing the relationships between the inertial, principal, and fluid film systems and is a view of the various coordinate systems as viewed along the direction of the system centerline, axis ζ. The system $X_n Y_n Z_n$ is fixed to shaft n.

Each of the rotors has an arbitrary tilt which can be represented by its magnitude, γ_n, measured about the axis x_n in the principal system of element n. The relative tilt between the two rotors is denoted by γ, and is measured about the 1 axis in the
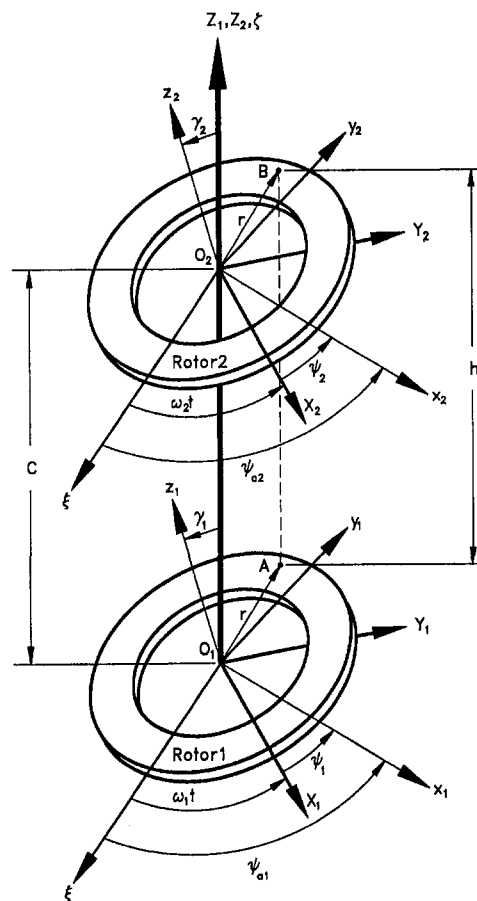

Fig. 2 FMRR seal kinematic model and coordinate systems

fluid film coordinate system described by Wileman and Green (1991). Because the rotor tilts are small, usually on the order of a milliradian, the relative tilt can be expressed as a vector subtraction of the individual rotor tilts by referring to Fig. 3. The resulting kinematic relationship is

$$\gamma = \gamma_2 \cos \phi_2 - \gamma_1 \cos \phi_1 \tag{1}$$

Nomenclature

a_k = coefficients of the Hurwitz polynomial

c_n = inertia ratio of element n, I_n/J_n

C_0 = equilibrium centerline clearance

d_{11} = fluid film damping coefficient, $2\pi R_m^3 G_0$

d_{s11}^* = support damping coefficient, angular mode

d_{s11} = dimensionless damping coefficient, $d^*\omega_{\text{ref}} C_0/Sr_o^4$

E_0 = stiffness parameter, $(1 - R_i)R_m/(2 + \beta(1 - R_i))$

G_0 = damping parameter, $\ln[1 + \beta(1 - R_i)] - 2\beta(1 - R_i)/[2 + \beta(1 - R_i)]/\beta^3(1 - R_i)^2$

I^* = dimensional transverse moment of inertia

I = normalized transverse moment of inertia, $I^*\omega_{\text{ref}}^2 C_0/Sr_o^4$

J^* = dimensional polar moment of inertia

J = normalized polar moment of inertia, $J^*\omega_{\text{ref}}^2 C_0/Sr_o^4$

k_{11} = fluid film direct stiffness coefficient, $\pi(P_o - P_i)(\beta R_i - 1)E_0^2$

k_{12} = fluid film cross-coupled stiffness coefficient, $d_{11}[\dot{\psi}_{ff} - (\omega_1 + \omega_2)/2]$

k_{sn}^* = support stiffness coefficient, element n

k = dimensionless stiffness coefficient, k^*C_0/Sr_o^4

M_n^* = moment applied to element n

M_n = normalized moment, M_n^*/Sr_0^3

p = pressure

P = normalized pressure, p/S

r = radius

R = normalized radius, r/r_o

S = seal parameter, $6\mu\omega_{\text{ref}}(r_o/C_0)^2(1 - R_i)^2$

t^* = time

t = normalized time, $\omega_2 t^*$

β^* = coning angle

β = normalized coning angle, $\beta^* r_o/C_0$

γ^* = relative tilt angle (radians)

γ_n^* = tilt angle of element n (radians)

γ = normalized tilt, $\gamma^* r_o/C_0$

λ = complex eigenvalue

μ = viscosity

ϕ_n = phase angle between element principal and fluid film systems

ψ_{ff} = absolute precession of fluid film system

ψ_n = relative precession angle

ψ_{an} = absolute precession angle

ω_n^* = shaft angular speed of element n

ω_n = normalized shaft speed, $\omega_n^*/\omega_{\text{ref}}$

ω_{ref} = reference shaft speed (Used for normalization)

ω_a = mean shaft speed

Subscripts

0 = equilibrium value

i = inner radius

k = term index in the characteristic equation

m = mean radius

n = element number ($n = 1$ or 2)

o = outer radius

where ϕ_1 and ϕ_2 represent relative precession angles between the principal systems and the fluid film system.

The moments applied by the fluid film are expressed in terms of this relative tilt and its time derivative using the rotor dynamic coefficients derived by Wileman and Green (1991). The flexible supports in a seal normally consist of springs and a secondary seal, such as an O-ring (Fig. 1). The moments applied by the support depend upon the motion of each element with respect to the shaft upon which it is mounted and are described in terms of linear stiffness and damping constants.

The equations of motion for the system are obtained by transforming the flexible support and fluid film moments into the inertial reference frame, then forming a moment balance between these applied moments and the dynamic moments. The resulting equations are linear in the kinematic variables, with harmonic forcing functions resulting from the initial misalignment of the flexible supports (Wileman and Green, 1997). These forcing functions do not affect the stability criteria of the system, which are obtained considering only the homogeneous equations of motion. Eliminating the forcing functions from the normalized equations of motion derived by Wileman and Green (1997), we obtain

$$I_2\ddot{\gamma}_{\xi 2} + d_2\dot{\gamma}_{\xi 2} - d_{11}\dot{\gamma}_{\xi 1} + J_2\omega_2\dot{\gamma}_{\eta 2} + k_2\gamma_{\xi 2}$$
$$- k_{11}\gamma_{\xi 1} + D_2\gamma_{\eta 2} - D_{11}\gamma_{\eta 1} = 0$$

$$I_2\ddot{\gamma}_{\eta 2} + d_2\dot{\gamma}_{\eta 2} - d_{11}\dot{\gamma}_{\eta 1} - J_2\omega_2\dot{\gamma}_{\xi 2} + k_2\gamma_{\eta 2}$$
$$- k_{11}\gamma_{\eta 1} - D_2\gamma_{\xi 2} + D_{11}\gamma_{\xi 1} = 0$$

$$I_1\ddot{\gamma}_{\xi 1} + d_1\dot{\gamma}_{\xi 1} - d_{11}\dot{\gamma}_{\xi 2} + J_1\omega_1\dot{\gamma}_{\eta 1} + k_1\gamma_{\xi 1}$$
$$- k_{11}\gamma_{\xi 2} + D_1\gamma_{\eta 1} - D_{11}\gamma_{\eta 2} = 0$$

$$I_1\ddot{\gamma}_{\eta 1} + d_1\dot{\gamma}_{\eta 1} - d_{11}\dot{\gamma}_{\eta 2} - J_1\omega_1\dot{\gamma}_{\xi 1} + k_1\gamma_{\eta 1}$$
$$- k_{11}\gamma_{\eta 2} - D_1\gamma_{\xi 1} + D_{11}\gamma_{\xi 2} = 0 \quad (2)$$

where the equations have been simplified using the following shorthand terms:

$$k_n = k_{11} + k_{sn}; \quad d_n = d_{11} + d_{sn}$$
$$D_n = \tfrac{1}{2}d_{11}(\omega_1 + \omega_2) + \omega_n d_{sn}$$
$$D_{11} = \tfrac{1}{2}d_{11}(\omega_1 + \omega_2)$$

Although the equations are linear, they are coupled by the fluid film and gyroscopic effects. The individual variables have been defined by Wileman and Green (1997) and are repeated in the nomenclature for reference.

Starting with these equations, the stability analysis can be approached in two different ways. To obtain stability criteria in closed form, it is necessary to make simplifying assumptions. The least severe of these which still results in a manageable solution is to neglect the support damping. A solution for the stability criteria in the absence of support damping is presented in Appendix A.

A general solution for the stability of Eqs. (2) can be obtained using a Routh-Hurwitz analysis (see, e.g., Appendix C of Arnold and Maunder, 1961). As described below, this solution can be used to make numeric computations of the stability limit for a seal in which all or most of the design and operating parameters are specified.
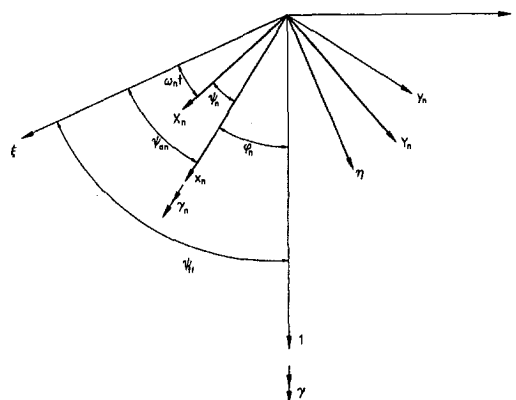

Fig. 3 Vector diagram showing relationship of coordinate axes for a single element as viewed along the system centerline

Stability Analysis Using the Routh-Hurwitz Criterion

When applied to the FMRR seal, the stability analysis will determine whether the system is stable for a given set of operating conditions. To employ the Routh-Hurwitz technique, it is first necessary to obtain the characteristic equation.

The ξ and η equations for each element can be combined using complex notation. Define the complex kinematic variables

$$g_2 = \gamma_{\xi 2} + i\gamma_{\eta 2}; \quad g_1 = \gamma_{\xi 1} + i\gamma_{\eta 1}$$

For each element multiply the η equation in (2) by i and add the ξ and η equations, substituting the definitions above. To obtain the characteristic equation, substitute a harmonic solution of the form

$$g_2 = g_{20}e^{\lambda t}; \quad g_1 = g_{10}e^{\lambda t}$$

where λ is a complex eigenvalue. In matrix form, the resulting equations are

$$\begin{pmatrix} \lambda^2 I_2 + \lambda(d_2 - iJ_2\omega_2) + (k_2 - iD_2) & -[\lambda d_{11} + (k_{11} - iD_{11})] \\ -[\lambda d_{11} + (k_{11} - iD_{11})] & \lambda^2 I_1 + \lambda(d_1 - iJ_1\omega_1) + (k_1 - iD_1) \end{pmatrix} \begin{Bmatrix} g_{20} \\ g_{10} \end{Bmatrix} = \begin{Bmatrix} 0 \\ 0 \end{Bmatrix} \quad (3)$$

Note that the two complex equations are still coupled. To obtain a nontrivial solution, the determinant of the matrix in (3) must be zero. Setting the determinant equal to zero yields a complex characteristic equation which is a fourth degree polynomial in λ. To obtain the real characteristic equation, or Hurwitz polynomial, it is necessary to multiply this equation by its complex conjugate. The resulting real equation will be the sum of the squares of the real and imaginary parts of the complex equation and will have the form

$$\sum_{k=0}^{8} a_k\lambda^k = 0 \quad (4)$$

The expressions for the coefficients a_k are presented in Appendix B.

Expanding the Hurwitz determinants symbolically yields unwieldy expressions. Instead, values are supplied for the design parameters of the seal so that the numerical values of the determinants can be computed. The coefficients a_k of (4) are computed using the expressions in Appendix B; then, the determinants are computed following the procedure of Arnold and Maunder (1961). If all eight of the determinants are positive, then the seal will be dynamically stable.

In addition to its utility for completely defined seals, the Routh-Hurwitz technique can also be useful for determining the acceptable range of a single design parameter if all of the others have been specified. This technique, described below, can be applied to the analysis of a single variable, or it can be applied to a succession of variables as in the parametric study which follows.

Parametric Study

To provide some insight into the general trends of how stability thresholds change with various design parameters, as well as to illustrate the technique developed above, a parametric study was performed upon an example seal. The example chosen is similar in design to that used by Green and Etsion (1986).

The parametric analyses were performed by substituting values for all of the variables in (4) except the shaft speed of element 2. The Hurwitz determinants were then expanded using a symbolic manipulator. The range of ω_2 for which all eight determinants were positive was then determined. This technique was first applied to the reference configuration, then one parameter at a time in the reference design was changed, and the effect of changing the value upon the acceptable range of ω_2 was determined. In each analysis, the parameters not being tested were maintained at their reference values, and for each parameter tested, one value higher than the reference value was tested and one value lower. Ten design parameters were tested in this way: the inertia ratio of element 2; the moments of inertia, support stiffness, and support damping of elements 1 and 2; the pressure drop across the seal; the coning angle; and the design clearance. The reference seal design was selected to be as symmetric as possible so that the effects of asymmetry in the system would not obscure the effects of the changes in the parameter values.

In the FMR analysis, Green (1989, 1990) showed that the behavior of the system changed dramatically as a function of the ratio of the transverse to the polar moment of inertia. If the value of this inertia ratio, $c_n = I_n/J_n$, approaches 1/2, meaning that the rotor is a short disk, then the gyroscopic moments in the system tend to align the rotor axis with the axis of rotation. If c is large, indicating a rotor which is long relative to its diameter, then the gyroscopic moments tend to make the rotor axis and the axis of rotation perpendicular. To test the effect of the change in c_n upon the system, the entire set of stability analyses was performed twice: once for $c_2 = 0.5$ and once for $c_2 = 3$. The value of c_1 was maintained at 0.5 for all of the analyses.

The results of the analyses are presented in Table 1. The leftmost columns represent the cases for which $c_2 = 0.5$, and the rightmost the cases for which $c_2 = 3$. For each parameter tested, the low, reference, and high values used for the analysis are given, followed by the range of values of ω_2 for which the system was stable. A negative shaft speed corresponds to rotation in the negative sense about axis ζ. The speed of element 1 was maintained constant at $\omega_1 = -2000$ rad/s. Thus, we expect some asymmetry in the results when we compare changes in properties for element 1 with changes in the corresponding properties for element 2.

When the speed of element 2 falls between the minimum and maximum values listed in the table, all of the determinants are positive, indicating a stable response. When rotor 2 falls below the minimum speed or exceeds the maximum speed, one or more of the determinants in the Routh-Hurwitz analysis is negative, indicating that the seal is unstable. Note that since ω_1 is always negative, results for counterrotating shafts correspond to positive values of ω_2 while corotating shafts correspond to negative values of ω_2. Note also that the middle result for each parameter in the table is always the reference case. The reference case result was repeated in the table for each variable to facilitate comparison and identification of trends. The outer ra-

dius, r_o, of the seal was 0.04 m; the dimensionless radius ratio of the seal, $R_i = r_i/r_o$, was 0.8; and the fluid viscosity, μ, was 5×10^{-4} Pa s.

Before examining the effects of the parameter changes individually, it is interesting to compare the general difference in stability range between the short and long rotor. Under almost all conditions, the stability range is larger for the case where both rotors are short. This indicates that Green's prediction that the gyroscopic moments in a short disk stabilize the FMR system can be generalized to the FMRR configuration. When $c_2 = 0.5$, the stable range of ω_2 is roughly centered about the value of ω_1; the stable operating range is larger for corotating ($\omega_2 < 0$) than for counterrotating ($\omega_2 > 0$) shafts. When $c_2 = 3$, the range of ω_2 for which the system is stable is no longer centered about the value of ω_1, but is skewed toward the counterrotating regime. The movement of the range toward counterrotating operation indicates that the increased fluid film stiffness in this regime transfers restoring moments from the short rotor to the long.

For the case where both elements are short disks, the stability range of the system decreases as the moment of inertia of element 1 increases. For the case where element 2 is a long rotor, the range of stability remains about the same, but the values are shifted toward the speed of element 1.

When both elements are short disks, the stability range increases slightly with the moment of inertia of element 2. When element 2 is a long rotor, the speed range for counterrotating seals is relatively unchanged while that for corotating seals decreases.

The stability range of the system is almost independent of the support stiffness of both elements, improving only slightly as a result of nearly doubling the stiffness of either support. This occurs because the fluid film stiffness is normally much larger than the support stiffness, typically by three orders of magnitude, so that the fluid film stiffness dominates the response.

The effect of the support damping is somewhat more pronounced, and its effect upon the stability range becomes very large as the damping approaches zero. The effect of decreasing the damping to zero is to dramatically reduce the stability range of counterrotating shafts except when the damping of a long element is zero, in which case the speed range increases dramatically. The effect of the damping upon corotating shafts is minimal, except for this same case, in which the range of stability is again increased dramatically.

For the case of two short disks, the effect of increasing the pressure drop was to increase the stability range for both counter and corotating shafts. When element 2 had a long rotor, however, increasing the pressure drop decreased the stability range of the counterrotating seal, but increased the stability range for the corotating seal.

The effect of the coning angle upon the stability of the system was relatively small. For the case of two short rotors, the stability range increased monotonically with coning angle, indicating that the primary mechanism involved is fluid damping. The maximum angular fluid stiffness occurs when $\beta = 12.5$, which corresponds to a dimensional coning angle of 3.13 milliradians. For the case of $c_2 = 3$, the speed range was maximum for this coning angle when the shafts corotate, indicating that the primary mechanism in this configuration is fluid stiffness. The effect upon counterrotating shafts was for this optimal coning to produce the smallest stability range.

The effect of design clearance was also relatively small. When both disks are short, there is an intermediate value of the clearance for which the stability range of the system is minimized. When one of the elements is long, the stability range for counterrotating shafts increased with clearance and the range for corotating shafts decreased.

The analysis above is based upon the linearized fluid-film stiffness and damping coefficients derived using the ``narrow

Table 1   Range of ω_2 for stable operation under various operating conditions

Variable (dimensional)	Value	$c_2 = 0.5$ (short rotor)			$c_2 = 3$ (long rotor)		
		Minimum speed (rad/s)	Maximum speed (rad/s)	Speed range (rad/s)	Minimum speed (rad/s)	Maximum speed (rad/s)	Speed range (rad/s)
I_1^* (kg m^2)	4.0E−04	−14,011.8	9,481.8	23493.6	−1,971.2	3,473.5	5444.8
	8.0E−04†	−10,901.8	6,024.2	16926.0	−2,816.1	2,776.3	5592.3
	1.2E−03	−9,628.3	4,460.3	14088.6	−3,289.4	2,554.8	5844.2
I_2^* (kg m^2)	4.0E−04	−10,629.2	4,174.1	14803.3	−4,149.5	2,704.6	6854.0
	8.0E−04†	−10,901.8	6,024.2	16926.0	−2,816.1	2,776.3	5592.3
	1.2E−03	−11,003.6	6,411.0	17414.6	−1,964.6	2,860.1	4824.7
k_{s1}^* (N m/rad)	100	−10,798.4	5,825.5	16623.9	−2,692.3	2,554.6	5246.9
	400†	−10,901.8	6,024.2	16926.0	−2,816.1	2,776.3	5592.3
	700	−11,003.8	6,203.6	17207.4	−2,930.9	2,985.7	5916.6
k_{s2}^* (N m/rad)	100	−10,900.7	5,994.9	16895.6	−2,602.4	2,445.8	5048.2
	400†	−10,901.8	6,024.2	16926.0	−2,816.1	2,776.3	5592.3
	700	−10,903.0	6,051.0	16954.0	−3,014.2	3,091.1	6105.3
d_{s1}^* (N m s/rad)	0	−10,216.9	274.3	10491.2	−2,561.9	242.9	2804.7
	0.24†	−10,901.8	6,024.2	16926.0	−2,816.1	2,776.3	5592.3
	0.48	−11,568.6	7,429.1	18997.7	−3,144.0	5,722.8	8866.8
d_{s2}^* (N m s/rad)	0	−10,916.2	860.4	11776.6	−14,277.6	9,479.3	23756.9
	0.24†	−10,901.8	6,024.2	16926.0	−2,816.1	2,776.3	5592.3
	0.48	−10,887.6	5,435.8	16323.4	−2,628.2	1,466.9	4095.0
$p_o - p_i$ (Pa)	5E+05	−9,125.8	4,644.2	13770.0	−2,438.7	3,033.8	5472.5
	1E+06†	−10,901.8	6,024.2	16926.0	−2,816.1	2,776.3	5592.3
	1.5E+06	−12,341.8	7,262.9	19604.7	−2,985.2	2,693.8	5679.0
β^* (rad)	1.56E−3	−10,069.6	4,924.8	14994.4	−2,802.6	2,813.5	5616.1
	3.13E−3†	−10,901.8	6,024.2	16926.0	−2,816.1	2,776.3	5592.3
	4.69E−3	−11,306.4	6,796.6	18103.0	−2,760.5	2,790.0	5550.5
C_0 (m)	5E−06	−12,754.0	6,727.4	19481.4	−3,173.3	2,652.6	5825.9
	1E−05†	−10,901.8	6,024.2	16926.0	−2,816.1	2,776.3	5592.3
	1.5E−05	−11,019.0	6,984.0	18003.0	−2,545.6	2,913.1	5458.7

† Reference Value.

seal'' approximation and other assumptions described in detail by Wileman and Green (1991). Only a comprehensive numerical analysis could determine the accuracy of the results presented here with respect to a complete nonlinear solution. However, the linearized coefficients obtained for the FMS case using identical assumptions (Green and Etsion, 1983, 1985) were shown to provide excellent agreement (less than four percent error) with the results of a complete numerical analysis (Green and Etsion, 1986), even in cases where the radius ratio, R_i, was as low as 0.7. Since the FMS seal is a special case of the FMRR configuration, it is reasonable to assume that the results presented in this work are equally accurate.

Conclusions

This work presented a derivation of the characteristic equation of an FMRR mechanical seal, and a stability analysis was performed upon this equation using the Routh-Hurwitz criterion. The method presented is a useful analytical tool for verifying that a seal design will be dynamically stable for a specified set of operating conditions.

The method was also used to examine the effect of changing various seal design parameters upon the stability of an example seal design. For the reference seal analyzed, the stability threshold was shown to depend strongly upon the ratio of the transverse to the polar moment of inertia. Rotors which have low inertia ratios, corresponding to short disks, benefit from the gyroscopic effect and are stable over much larger ranges of shaft speed than long rotors. In systems with a long rotor, the stable speed range is skewed toward the counterrotating regime, indicating that the increased fluid stiffness of this regime transfers restoring moments from the short rotor to the long. In seals with two short rotors, increasing fluid stiffness decreases the stable operating range. The gyroscopic effects tend to stabilize both rotors independently, and the optimum performance is obtained by minimizing the fluid coupling between them. In general, the fluid pressure, coning angle, and face clearance influenced the stability range much more than the support stiffness and damping. This implies that relatively more effort should be devoted to the fluid film effects than to the support effects during the design process.

A closed-form stability criterion was presented for the special case in which support damping is absent in the seal. The resulting closed-form stability results for the FMSR configuration degenerate to those found in the literature for the FMR configuration, demonstrating the consistency of the more general analysis presented here with a previous analysis for the FMR configuration.

It should be noted that while dynamic stability is necessary to prevent failure of a seal in operation, a stable seal may still fail as a result of a large steady-state misalignment, which may lead to either excessive leakage or face contact. Thus, both the stability and the steady-state response must be determined in order to verify that a seal design will have acceptable dynamic performance.

References

Allaire, P. E., 1984, "Noncontacting Face Seals for Nuclear Applications—A Literature Review," *Lubrication Engineering*, Vol. 40, No. 6, pp. 344–351.

Arnold, R. N., and Maunder, L., 1961, *Gyrodynamics and its Engineering Applications*, Academic Press, New York.

Etsion, I., 1982, "A Review of Mechanical Face Seal Dynamics," *The Shock and Vibration Digest*, Vol. 14, No. 2, pp. 9–14.

Etsion, I., 1985, "Mechanical Face Seal Dynamics Update," *The Shock and Vibration Digest*, Vol. 17, No. 4, pp. 11–15.

Etsion, I., 1991, "Mechanical Face Seal Dynamics 1985-1989," *The Shock and Vibration Digest,* Vol. 23, No. 4, pp. 3-7.

Green, I., and Etsion, I., 1983, "Fluid Film Dynamic Coefficients in Mechanical Face Seals," ASME JOURNAL OF LUBRICATION TECHNOLOGY, Vol. 105, pp. 297-302.

Green, I., and Etsion, I., 1985, "Stability Threshold and Steady-State Response of Noncontacting Coned-Face Seals," *ASLE Transactions,* Vol. 28, No. 4, pp. 449-460.

Green, I., and Etsion, I., 1986, "Nonlinear Dynamic Analysis of Noncontacting Coned-Face Mechanical Seals," *ASLE Transactions,* Vol. 29, No. 3, pp. 383-393.

Green, I., 1989, "Gyroscopic and Support Effects on the Steady-State Response of a Noncontacting Flexibly Mounted Rotor Mechanical Face Seal," ASME JOURNAL OF TRIBOLOGY, Vol. 111, pp. 200-208.

Green, I., 1990, "Gyroscopic and Damping Effects on the Stability of a Non-contacting Flexibly-Mounted Rotor Mechanical Face Seal," *Dynamics of Rotating Machinery,* Hemisphere Publishing Company, pp. 153-173.

Metcalfe, R., 1981, "Dynamic Tracking of Angular Misalignment in Liquid-Lubricated End-Face Seals," *ASLE Transactions,* Vol. 24, No. 4, pp. 509-526.

Miner, J. R., et al., 1992, "High Speed Seal Development, Part I," United Technologies, Pratt and Whitney, Interim Report to Wright Laboratory, Air Force Materiel Command, WL-TR-92-2101.

Person, V., Tournerie, B., and Frêne, J., 1997, "A Numerical Study of the Stable Dynamic Behavior of Radial Face Seals with Grooved Faces," accepted for publication in ASME JOURNAL OF TRIBOLOGY.

Tournerie, B., and Frêne, J., 1985, "Les joints d'étanchéité à faces radiales: étude bibliographique," *Matériaux Mécanique Électricité,* No. 410, pp. 44-52.

Wileman, J. M., and Green, I., 1991, "The Rotordynamic Coefficients of Mechanical Seals Having Two Flexibly Mounted Rotors," ASME JOURNAL OF TRIBOLOGY, Vol. 113, No. 4, pp. 795-804.

Wileman, J. M., and Green, I., 1996, "The Rotor Dynamic Coefficients of Eccentric Mechanical Face Seals," ASME JOURNAL OF TRIBOLOGY, Vol. 118, No. 1, pp. 215-224.

Wileman, J. M., and Green, I., 1997, "Steady-State Analysis of Mechanical Seals with Two Flexibly Mounted Rotors," ASME JOURNAL OF TRIBOLOGY, Vol. 119, No. 1, pp. 200-204.

Wileman, J. M., 1994, "Dynamic Analysis of Eccentric Mechanical Face Seals," Doctoral Dissertation, Georgia Institute of Technology.

APPENDIX A

Stability Analysis in the Absence of Support Damping

The analysis presented above is capable of analyzing the most general seal configuration. Although it is an entirely analytical approach, the final stage of the investigation was performed parametrically because the symbolic result cannot be presented as a single expression in closed form. However, with some suitable simplifications we can use a different technique to examine the stability behavior of the system for the special situation in which there is no support damping. Most seals contain support damping, so that this solution will not be directly applicable to them. The solution may be applicable, however, to seals which use a metal bellows for the secondary seal, as the damping in such seals is often very small. More importantly, though, the simple stability criterion which results from the analysis below allows quick comparison of the stability criteria for different seal configurations, and provides insight into the underlying physics of the problem.

To perform this simplified analysis, it is first necessary to express the equations of motion in the element principal systems. That is, the equations which represent the moment balance for element n are expressed in the principal system of element n. For small tilts, each of these transformations represents a simple rotation about the ζ axis; i.e., about the shaft centerlines.

To resolve the moments expressed in the inertial equations into components in the principal system, we use the rotation transformation

$$\begin{Bmatrix} M_{in} \\ M_{jn} \end{Bmatrix} = \begin{pmatrix} \cos \psi_{an} & \sin \psi_{an} \\ -\sin \psi_{an} & \cos \psi_{an} \end{pmatrix} \begin{Bmatrix} M_\xi \\ M_\eta \end{Bmatrix} \qquad (5)$$

This transformation is performed upon the first two equations of (2) using ψ_{a2} and on the last two using ψ_{a1}. In addition, the tilts in the principal systems are related to those in the inertial system using

$$\gamma_{\xi n} = \gamma_n \cos \psi_{an}; \quad \gamma_{\eta n} = \gamma_n \sin \psi_{an} \qquad (6)$$

The resulting general equations of motion in the element principal systems are presented by Wileman (1994).

The stability analysis is performed by examining the behavior of the system at its stability threshold, the condition at which a disturbance in the system will remain indefinitely, neither decaying nor growing. At stability threshold, assume that forcing functions are absent from the system, so that the dynamic response is due only to disturbances. Assume that the absolute tilt rates, which are measured in the element principal systems, are constant. Thus,

$$\dot{\gamma} = \dot{\gamma}_2 = \dot{\gamma}_1 = 0 \qquad (7)$$

Also, assume that the second derivatives of all of the precession variables are zero:

$$\ddot{\psi}_{a2} = \ddot{\psi}_{a1} = \ddot{\psi}_{ff} = 0 \qquad (8)$$

Equations (7) and (8) define a condition known as steady-state precession. A disturbance applied to such a system will produce a constant tilt which precesses at a constant rate and which remains in the system indefinitely.

When the tilts are assumed to be constant, the time derivative of the relative misalignment, γ, defined in (1) is

$$\gamma_2 \dot{\phi}_2 \sin \phi_2 - \gamma_1 \dot{\phi}_1 \sin \phi_1 = 0 \qquad (9)$$

As defined previously, the relative tilt in the fluid film system occurs about the 1 axis; i.e., there is no component of the relative tilt about the 2 axis. From Fig. 3, this can be seen to imply the kinematic identity

$$\gamma_2 \sin \phi_2 - \gamma_1 \sin \phi_1 = 0 \qquad (10)$$

Comparing (10) to (9) indicates that $\dot{\phi}_2 = \dot{\phi}_1$ must be satisfied, and this implies that $\dot{\psi}_{a2} = \dot{\psi}_{a1}$.

To obtain the equations of motion for steady-state precession, (7) to (9) are substituted into the general equations of motion in the element principal systems, along with $d_{s1} = d_{s2} = 0$ to neglect the support damping. The equations of motion at stability threshold are then

$$-I_2 \gamma_2 \dot{\psi}_{a2}^2 + J_2 \gamma_2 \omega_2 \dot{\psi}_{a2} = -k_{11} \gamma \cos \phi_2$$
$$- d_{11} [\dot{\psi}_{ff} - \tfrac{1}{2}(\omega_1 + \omega_2)] \gamma \sin \phi_2 - k_{s2} \gamma_2 \qquad (11a)$$

$$0 = -k_{11} \gamma \sin \phi_2 - d_{11}[\dot{\psi}_{ff} - \tfrac{1}{2}(\omega_1 + \omega_2)] \gamma \cos \phi_2 \qquad (11b)$$

$$-I_1 \gamma_1 \dot{\psi}_{a1}^2 + J_1 \gamma_1 \omega_1 \dot{\psi}_{a1} = k_{11} \gamma \cos \phi_1$$
$$+ d_{11}[\dot{\psi}_{ff} - \tfrac{1}{2}(\omega_1 + \omega_2)] \gamma \sin \phi_1 - k_{s1} \gamma_1 \qquad (11c)$$

$$0 = k_{11} \gamma \sin \phi_1 + d_{11}[\dot{\psi}_{ff} - \tfrac{1}{2}(\omega_1 + \omega_2)] \gamma \cos \phi_1 \qquad (11d)$$

If we neglect the trivial solution, $\gamma = 0$, then (11b) and (11d) can be divided by γ. The resulting equations can be satisfied simultaneously only when $\phi_1 = \phi_2$, which implies that the two elements have the same nutation axis as the fluid film system, so that

$$\phi_2 = \phi_1 = \dot{\phi}_2 = \dot{\phi}_1 = 0 \qquad (12)$$

Substituting (12) into either (11b) or (11d) yields the precession rate of the fluid film system, which will also be the absolute precession rate for each element:

$$\dot{\psi}_{ff} = \dot{\psi}_a = \tfrac{1}{2}(\omega_1 + \omega_2) \qquad (13)$$

Further, substituting (12) into (1) yields a simplified definition of γ:

$$\gamma = \gamma_2 - \gamma_1 \qquad (14)$$

Note that the absolute precession rate is equal (in the absence

of support damping) to the average of the two shaft speeds. Thus, it will be convenient to define a variable for this value:

$$\omega_a = \tfrac{1}{2}(\omega_1 + \omega_2) \qquad (15)$$

To simplify $(11a)$ and $(11c)$, substitute (12) to (15) to obtain

$$
\begin{pmatrix}
-I_2\dot\psi_a^2 + J_2\omega_2\dot\psi_a + (k_{11} + k_{s2}) & -k_{11} \\
-k_{11} & -I_1\dot\psi_a^2 + J_1\omega_1\dot\psi_a + (k_{11} + k_{s1})
\end{pmatrix}
\begin{Bmatrix} \gamma_2 \\ \gamma_1 \end{Bmatrix} = 0 \quad (16)
$$

A nontrivial solution requires that the determinant equal zero, yielding the stability criterion for the FMRR configuration in the absence of support damping:

$$I_1 I_2 \dot\psi_a^4 - (I_2 J_1 \omega_1 + I_1 J_2 \omega_2)\dot\psi_a^3$$

$$+ [J_1\omega_1 J_2\omega_2 - I_1(k_{11} + k_{s2}) - I_2(k_{11} + k_{s1})]\dot\psi_a^2$$

$$+ [J_1\omega_1(k_{11} + k_{s2}) + J_2\omega_2(k_{11} + k_{s1})]\dot\psi_a$$

$$+ (k_{11} + k_{s2})(k_{11} + k_{s1}) - k_{11}^2 = 0 \quad (17)$$

For a particular seal design, (17) is solved for $\dot\psi_a$, which imposes a condition upon the relationship between the two shaft speeds according to (13). Thus, for example, if ω_1 is prescribed then the value of ω_2 at the stability threshold can be determined. Equation (17) represents a closed-form stability criterion. Naturally, its results are identical to those obtained using the Routh-Hurwitz analysis when $d_{s1} = d_{s2} = 0$.

To compute the stability criterion for the FMSR configuration, in which one of the shafts does not rotate, substitute $\omega_1 = 0$ and $\omega_2 = 2\omega_a$ in (13), then substitute the result for $\dot\psi_a$ in (17). The stability criterion for the FMSR configuration becomes

$$I_1 I_2 \omega_a^4 - I_1 J_2\omega_2 \omega_a^3 - [I_1(k_{11} + k_{s2}) + I_2(k_{11} + k_{s1})]\omega_a^2$$

$$+ J_2\omega_2(k_{11} + k_{s1})\omega_a + k_{11}k_{s1} + k_{11}k_{s1} + k_{s2}k_{s1} = 0 \quad (18)$$

Now it is possible to compare the degenerate form of the FMSR stability criterion to the result derived previously for the FMR case. For element 1 (the stator) of the FMSR configuration to be rigidly constrained requires that the support stiffness for element 1 go to infinity. Solving (18) for k_{s1} yields

$$k_{s1} = \frac{I_1 I_2 \omega_a^4 - I_1 J_2\omega_2 \omega_a^3 - [(I_1 + I_2)k_{11} + I_1 k_{s2}]\omega_a^2 + k_{11}k_{s2}}{I_2\omega_a^2 - (k_{11} + k_{s2}) - 2J_2\omega_a}$$

$$(19)$$

k_{s1} approaches infinity as the denominator in (19) approaches zero. Thus, the stability criterion which satisfies the constraint that element 1 be rigidly mounted is

$$I_2\omega_a^2 - (k_{11} + k_{s2}) - 2J_2\omega_a = 0 \qquad (20)$$

This expression is equivalent to the stability criterion derived by Green (1990) for the equivalent FMR configuration. Note that because of the rigidity constraint on element 1, none of the properties of element 1 appears in (20). Particularly note that the inertia properties of element 1 appear only in the numerator

of the expression for k_{s1} in (19) and do not affect the stability criterion.

APPENDIX B

Coefficients of the Hurwitz Polynomial

The coefficients a_k in Eq. (21) are as follows:

$$a_8 = I_1^2 I_2^2$$

$$a_7 = 2I_1 I_2 (I_2 d_1 + I_1 d_2)$$

$$a_6 = (I_2 d_1 + I_1 d_2)^2 + (I_2 J_1 \omega_1 + I_1 J_2 \omega_2)^2$$
$$+ 2I_1 I_2 (I_2 k_1 + d_2 d_1 - J_2\omega_2 J_1\omega_1 + I_1 k_2 - d_{11}^2)$$

$$a_5 = 2(I_2 d_1 + I_1 d_2)(I_2 k_1 + d_2 d_1 - J_2\omega_2 J_1\omega_1 + I_1 k_2 - d_{11}^2)$$
$$+ 2I_1 I_2 (d_2 k_1 - D_1 J_2\omega_2 + d_1 k_2 - D_2 J_1\omega_1 - 2d_{11}k_{11})$$
$$+ 2(I_2 J_1\omega_1 + I_1 J_2\omega_2)(I_2 D_1 + J_2\omega_2 d_1 + J_1\omega_1 d_2 + I_1 D_2)$$

$$a_4 = (I_2 k_1 + d_2 d_1 - J_2\omega_2 J_1\omega_1 + I_1 k_2 - d_{11}^2)^2$$
$$+ 2(I_2 d_1 + I_1 d_2)(d_2 k_1 - D_1 J_2\omega_2$$
$$+ d_1 k_2 - D_2 J_1\omega_1 - 2d_{11}k_{11})$$
$$+ 2I_1 I_2 (k_2 k_1 - D_2 D_1 - k_{11}^2 + D_{11}^2)$$
$$+ (I_2 D_1 + J_2\omega_2 d_1 + J_1\omega_1 d_2 + I_1 D_2)^2$$
$$+ 2(I_2 J_1\omega_1 + I_1 J_2\omega_2)(J_2\omega_2 k_1 + D_1 d_2$$
$$+ J_1\omega_1 k_2 + D_2 d_1 - 2d_{11}D_{11})$$

$$a_3 = 2(I_2 J_1\omega_1 + I_1 J_2\omega_2)(D_2 k_1 + D_1 k_2 - 2k_{11}D_{11})$$
$$+ 2(I_2 D_1 + J_2\omega_2 d_1 + J_1\omega_1 d_2 + I_1 D_2)$$
$$\times (J_2\omega_2 k_1 + D_1 d_2 + J_1\omega_1 k_2 + D_2 d_1 - 2d_{11}D_{11})$$
$$+ 2(I_2 d_1 + I_1 d_2)(k_2 k_1 - D_2 D_1 - k_{11}^2 + D_{11}^2)$$
$$+ 2(I_2 k_1 + d_2 d_1 - J_2\omega_2 J_1\omega_1 + I_1 k_2 - d_{11}^2)$$
$$\times (d_2 k_1 - D_1 J_2\omega_2 + d_1 k_2 - D_2 J_1\omega_1 - 2d_{11}k_{11})$$

$$a_2 = (d_2 k_1 - D_1 J_2\omega_2 + d_1 k_2 - D_2 J_1\omega_1 - 2d_{11}k_{11})^2$$
$$+ 2(I_2 k_1 + d_2 d_1 - J_2\omega_2 J_1\omega_1 + I_1 k_2 - d_{11}^2)$$
$$\times (k_2 k_1 - D_2 D_1 - k_{11}^2 + D_{11}^2)$$
$$+ (J_2\omega_2 k_1 + D_1 d_2 + J_1\omega_1 k_2 + D_2 d_1 - 2d_{11}D_{11})^2$$
$$+ 2(I_2 D_1 + J_2\omega_2 d_1 + J_1\omega_1 d_2 + I_1 D_2)$$
$$\times (D_2 k_1 + D_1 k_2 - dk_{11}D_{11})$$

$$a_1 = 2(d_2 k_1 - D_1 J_2\omega_2 + d_1 k_2 - D_2 J_1\omega_1 - 2d_{11}k_{11})$$
$$\times (k_2 k_1 - D_2 D_1 - k_{11}^2 + D_{11}^2)$$
$$+ 2(J_2\omega_2 k_1 + D_1 d_2 + J_1\omega_1 k_2 + D_2 d_1 - 2d_{11}D_{11})$$
$$\times (D_2 k_1 + D_1 k_2 - 2k_{11}D_{11})$$

$$a_0 = (k_2 k_1 - D_2 D_1 - k_{11}^2 + D_{11}^2)^2$$
$$+ (D_2 k_1 + D_1 k_2 - 2k_{11}D_{11})^2$$